Int. J. Morphol.,
44(1):258-275, 2026.

Neuroregenerative Impact of Dipeptidyl Peptidase IV Inhibitor (Sitagliptin) on Median Nerve Injury in Rats: Biochemical, Histological, and Immunohistochemical Methodology

Impacto Neurorregenerativo del Inhibidor de la Dipeptidil Peptidasa IV (Sitagliptina) en la Lesión del Nervio Mediano en Ratas: Metodología Bioquímica, Histológica e Inmunohistoquímica

Rasha M. Salama & Omyma Ibraheem Zedan

SALAMA, R. M. & ZEDAN, O. I. Neuroregenerative impact of dipeptidyl peptidase IV inhibitor (sitagliptin) on median nerve injury in rats: Biochemical, histological, and immunohistochemical methodology. *Int. J. Morphol., 44(1)*:258-275, 2026.

SUMMARY: Peripheral nerve injury is frequently associated with incomplete functional recovery despite surgical intervention. Sitagliptin, a dipeptidyl peptidase-4 inhibitor, has shown anti-inflammatory, antioxidant, and anti-apoptotic qualities in a number of animal models. This study was designed to evaluate the potential neuroregenerative effect of sitagliptin following median nerve crush injury in rats. Forty-eight adult male albino rats were randomly assigned into eight groups, including sham-operated, sitagliptin-treated, median nerve injury, and median nerve injury treated with sitagliptin groups, evaluated at 7 and 28 days. Sitagliptin was orally administered at a dose of 10 mg/kg/day. Biochemical assessment included oxidative stress markers, antioxidant enzymes, inflammatory cytokines, and nerve growth factor. Hematoxylin and eosin and Masson's trichrome were used for the histological evaluation, while immunohistochemical analysis assessed GFAP, Nrf2, and BAX expression. Median nerve crush injury at 7 days (MNI-7 group) resulted in marked oxidative stress, inflammatory response, apoptosis, structural nerve disruption, and collagen deposition, accompanied by reduced nerve growth factor levels. While, MNI-28 group unambiguously illustrated some improvement in all measured parameters. Sitagliptin treatment significantly attenuated lipid peroxidation, restored antioxidant enzyme activity, reduced inflammatory markers, and increased nerve growth factor levels. Histological and immunohistochemical findings demonstrated improved nerve architecture, reduced fibrosis, decreased GFAP and BAX immunoreactivity, and enhanced Nrf2 expression, particularly with prolonged treatment. These findings indicate that sitagliptin promotes biochemical and structural recovery following median nerve crush injury, likely through its anti-inflammatory, antioxidant, and anti-apoptotic properties, pointing to a possible medicinal use in promoting peripheral nerve regeneration.

KEY WORDS: Peripheral nerve injury; Sitagliptin; Oxidative stress; GFAP; Nrf2; BAX.

INTRODUCTION

Peripheral nerve injury (PNI) represents a serious and highly prevalent global health problem that substantially compromises patients' quality of life. Depending on the severity and extent of injury, PNI may result in partial or complete loss of motor function in the innervated organs, sensory disturbances, chronic neuropathic pain, and, in severe cases, permanent functional disability (Faroni *et al*., 2015; Li *et al*., 2019). The most common etiologies of peripheral nerve injuries include road traffic accidents, gunshot wounds, penetrating trauma, traction injuries, and crush injuries (Alvites *et al*., 2018).

Among these mechanisms, crush injury constitutes one of the most frequently encountered forms of peripheral nerve trauma. Such injury occurs when a blunt compressive force—commonly produced by instruments such as surgical clamps—acts on the nerve without causing complete transection. Crush injuries may also arise from high-impact events, including motor vehicle collisions or blunt assault (Caillaud *et al*., 2019).

In contrast to the central nervous system neurons, neurons of the peripheral nervous system possess a limited intrinsic capacity for regeneration following injury. Nevertheless, restoration of normal structure and function after PNI remains a major clinical challenge for orthopedic, plastic, and reconstructive surgeons (Houschyar *et al*., 2016). Axonal regeneration after peripheral nerve injury is often slow, incomplete, and inefficient, frequently resulting in irreversible structural and functional deterioration of

Department of Anatomy and Embryology, Faculty of Medicine, Menoufia University, Egypt.

Received: 2025-10-08 Accepted: 2025-12-20

target organs before effective reinnervation can be achieved (Li *et al.*, 2019). Consistent with this, numerous clinical reports over recent years have demonstrated that postoperative functional recovery—particularly motor recovery—following peripheral nerve injury remains suboptimal (Li *et al*., 2019). Accordingly, there is a compelling need to identify novel therapeutic approaches capable of accelerating nerve regeneration and improving functional outcomes.

Inhibitors of dipeptidyl peptidase-4 (DPP-4), such as sitagliptin (STG), are FDA-approved oral hypoglycemic agents that enhance insulin secretion and suppress glucagon release (Huang *et al*., 2022). Sitagliptin was first approved for the treatment of type II diabetes mellitus in the United States in October 2006 and subsequently by the European Medicines Agency in 2007 at a standard daily dose of 100 mg. The drug is generally well tolerated, with predominantly mild to moderate adverse effects reported (Karagiannis *et al*., 2014).

Pharmacologically, sitagliptin acts through competitive inhibition of the DPP-4 enzyme, a membrane-bound aminopeptidase presents in plasma that plays a critical role in glucose homeostasis and inflammatory regulation. DPP-4 mediates the degradation of the incretin hormones gastric inhibitory polypeptide, and glucagon-like peptide-1. By preventing the breakdown of these peptides, sitagliptin prolongs their biological activity, leading to enhanced insulin secretion, reduced glucagon release from pancreatic a-cells, and subsequent normalization of blood glucose levels (Ezzeddini *et al*., 2019).

Beyond its established antidiabetic efficacy, growing evidence suggests that sitagliptin exerts beneficial effects in a variety of pathological conditions, including cardiac, renal, pulmonary, intestinal, pancreatic, and gastrointestinal injuries, as well as ischemic stroke (Bassendine *et al*., 2020; Huang *et al*., 2022). These pleiotropic effects have largely been attributed to the potent antioxidant, anti-inflammatory, anti-apoptotic, and neuroregenerative properties of sitagliptin, mediated through preservation of endogenous antioxidant defenses and attenuation of free radical generation.

As far as we comprehend, the possible neuroregenerative effects of sitagliptin in peripheral nerve injury have not yet been investigated. Therefore, the objective of the current study was to assess, for the first time, the antioxidant, anti-inflammatory, anti-apoptotic, and neuroregenerative effects of sitagliptin in an experimental model of median nerve crush injury.

MATERIAL AND METHOD

Animals

Forty-eight healthy adult male albino rats, approximately 8 weeks of age and weighing 250 ± 50 g, were obtained from the animal house of Kasr El-Aini Faculty of Medicine, Cairo University. Animals were housed under standardized laboratory conditions, including controlled temperature, humidity, and a 12-hour light/dark cycle, with unrestricted access to standard laboratory chow and tap water. Before the experimental procedures began, there was a one-week acclimatization phase to minimize stress-related variability.

All experimental procedures were approved by the Institutional Scientific Research Ethics Committee, Faculty of Medicine, Menoufia University (IRB approval number: 6/2025ANT4), and were carried out in compliance with accepted international standards for the handling and care of lab animals.

Surgical median nerve crush injury procedure

Rats were anesthetized by intraperitoneal injection of ketamine hydrochloride (100 mg/kg) combined with xylazine (20 mg/kg). Adequate anesthesia was confirmed by the absence of withdrawal reflexes. Following shaving of the operative area and application of aseptic techniques, a longitudinal skin incision was made along the medial aspect of the right forelimb.

The right median nerve was carefully exposed approximately 10 mm proximal to the elbow joint. A standardized crush injury was induced using a conventional hemostatic forceps applied at the second notch for a duration of two minutes, ensuring uniform compression without complete nerve transection. After the injury, the nerve was repositioned, and the skin incision was closed using 4-0 silk sutures, as previously described by Santos *et al*. (2012).

Experimental substances

Sitagliptin (STG) tablets (Januvia®, 100 mg) were obtained from Merck & Co., Inc. (Kenilworth, NJ, USA). STG was freshly prepared by dissolving the required dose in distilled water. The experimental dose of STG was 10 mg/kg/day, administered orally via gastric gavage in a volume of 0.1 mL/100 g body weight, in accordance with previously validated experimental protocols (Kizilay *et al*., 2021).

Experimental design

The forty-eight rats were randomly allocated into eight experimental groups (n = 6 rats per group) as follows:

I. **Sham-7 group:** A surgical incision was performed without median nerve compression, and the wound was closed on day 1 of the experiment. Rats were sacrificed on day 7.
II. **Sham-28 group:** A surgical incision was performed without median nerve compression, and the wound was closed on day 1 of the experiment. Rats were sacrificed on day 28.
III. **STG-7 group:** Sitagliptin was given orally at a dose of 10 mg/kg/day, dissolved in 0.1 mL/100 g distilled water, from day 1 of the experiment for 7 days. Rats were sacrificed on day 7.
IV. **STG-28 group:** Sitagliptin was given orally at a dose of 10 mg/kg/day, dissolved in 0.1 mL/100 g distilled water, from day 1 of the experiment for 28 days. Rats were sacrificed on day 28.
V. **MNI-7 group:** Median nerve crush injury was induced on day 1 of the experiment, after which the incision was closed. Rats were sacrificed on day 7.
VI. **MNI-28 group:** Median nerve crush injury was induced on day 1 of the experiment, after which the incision was closed. Rats were sacrificed on day 28.
VII. **MNI & STG-7 group:** Median nerve crush injury was induced on day 1 of the experiment, followed by oral administration of sitagliptin (10 mg/kg/day) for 7 days. Rats were sacrificed on day 7.
VIII. **MNI & STG-28 group:** Median nerve crush injury was induced on day 1 of the experiment, followed by oral administration of sitagliptin (10 mg/kg/day) for 28 days. Rats were sacrificed on day 28.

Evaluation methods

Biochemical analysis

The animals were fasted overnight at the conclusion of the trial. Each rat's tail vein was used to draw blood, which was then left to clot for 30 minutes at room temperature. After that, samples were centrifuged for 15 minutes at 2000 rpm. Prior to biochemical examination, the separated serum was collected and kept at -80 °C (Nemzek *et al*., 2001).

The following serum parameters were assessed:

1. **Malondialdehyde (MDA):** Assessed as a measure of oxidative stress and lipid peroxidation.
2. **Glutathione (GSH), Superoxide dismutase (SOD), Catalase (CAT), and Glutathione peroxidase (GPx):** Evaluated as indicators of antioxidant defense and oxidative stress status.
3. **Interleukin-6 (IL-6) and Tumor necrosis factor-α (TNF-α):** Appraised as indices of systemic inflammatory response.
4. **Nerve growth factor (NGF):** Assessed as a biochemical marker of neuronal regeneration following injury.

Histological and immunohistochemical studies

Rats were sacrificed at the conclusion of the experiment, and specimens of median nerves were meticulously dissected. Samples were processed normally, fixed in 10 % formol saline for a full day, and embedded in paraffin wax. Paraffin blocks were sectioned at a thickness of 5 µm for light microscopic examination (Suvarna *et al*., 2019).

I. Histological studies (Suvarna *et al*., 2019):

1. Hematoxylin and Eosin (H&E) stain: Used to evaluate the general histological architecture of the median nerve.
2. Masson's Trichrome stain: Applied to assess collagen fiber distribution and deposition.

II. Immunohistochemical studies

Immunohistochemical staining was performed using the labeled avidin–biotin peroxidase technique (Bancroft & Gamble, 2008) to detect the immunoexpression of the following markers:

- **Glial fibrillary acidic protein (GFAP):** Used as a marker for Schwann cell (Neurolemmocyte) activation and neuroglial response following nerve injury (Farahani *et al*., 2022).
- **Nuclear factor erythroid 2-related factor 2 (Nrf2):** Evaluated as a marker of antioxidant defense and oxidative stress response (Oh & Jun, 2017).
- **BAX**: Assessed as a marker of apoptosis, representing pro-apoptotic signaling pathways within injured nerve tissue (Zhang *et al*., 2014).

Appropriate positive and negative controls were included in all immunohistochemical procedures.

Morphometrical analysis

Morphometric evaluation was performed using an image analyzer system (Leica Q500 MC, Leica Microsystems, Germany) at the Anatomy Department, Faculty of Medicine, Menoufia University. Five non-

overlapping fields per section were examined at ×400 magnification.

The following parameters were quantified:

- Mean area percent of collagen fiber deposition in Masson's trichrome-stained sections
- Mean area percent of positive immunoreactivity for GFAP
- Mean area percent of positive immunoreactivity for Nrf2
- Mean area percent of positive immunoreactivity for BAX

Statistical analysis

The Statistical Package for Social Sciences (SPSS) version 27 (SPSS Inc., Chicago, IL, USA) was used to statistically analyze the collected data. The range and mean ± standard deviation were used to express quantitative variables. Group comparisons were performed using the Mann–Whitney U test. Statistical significance was defined as a p-value of less than 0.05.

RESULTS

No statistically significant differences were detected among the Sham-7, Sham-28, STG-7, and STG-28 groups across all evaluated biochemical, histological, immunohistochemical, and morphometric parameters. Accordingly, these groups were considered collectively as the control group for subsequent comparisons.

Serum Biochemical results

Lipid peroxidation and oxidative stress markers

Serum MDA levels showed a highly significant increase in the MNI-7, MNI-28, and MNI & STG-7 groups when compared to the control group ($P < 0.001$). When compared with the MNI-7 group, MDA levels were significantly reduced in the MNI-28 and MNI & STG-7 groups ($P = 0.004$ and $P = 0.009$, respectively). The MNI & STG-28 group demonstrated a highly significant decrease

Table I. Serum biochemical lipid peroxidation and oxidative stress markers in the studied groups.

	Studied groups				
	Control	**MNI-7**	**MNI-28**	**MNI & STG-7**	**MNI & STG-28**
1. Malondialdehyde (MDA) nmol/ml	42.83±9.33	148.67±18.63	104.67±9.46	91.92±5.64	54.01±9.31
Mean ±SD	33 – 60	129 – 170	88.9 – 117.8	85.2 – 98.1	40.3 – 63.10
Range					
Test		4.5[1]	3.8[1]	3.6[1]	1.59[1]
P value		<0.001[1]	<0.001[1]	<0.001[1]	0.06[1]
			0.004[2]	0.009[2]	<0.001[2]
2. Glutathione (GSH) mmol/ml	152.05±21.10	62.32±8.88	102.28±9.82	119.12±20.51	133.22±9.55
Mean ±SD	129.8 – 187	52.3 – 75.4	89.1 – 115.8	95.6 – 139.5	119.5 – 144.9
Range					
Test		3.10[1]	2.88[1]	2.01[1]	1.60[1]
			2.31[2]	2.66[2]	2.98
P value		<0.001[1]	<0.008[1]	0.045[1]	0.11[1]
3. Superoxide dismutase (SOD) u/ml	57.23±10.21	20.1±7.73	32.5±7.68	39.33±10.53	45.10±9.86
Mean ±SD	45.6 – 73.5	9.7 – 30.2	20.1 – 42.5	39.6 – 57	33.9 – 60.7
Range					
Test		3.66[1]	2.71[1]	2.41[1]	1.76[1]
			2.08[2]	2.57	3.11
P value		<0.001[1]	0.008[1]	0.2[1]	0.08[1]
			0.037[2]	0.007[2]	<0.001[2]
4. Catalase (CAT) u/ml	232.9±19.34	113.18±20.12	177.23±17.60	202.13±13.30	227.90±12.96
Mean ±SD	216.5 – 269.8	90.5 – 140.1	146.5 – 201.5	185.6 – 217.8	213.3 – 240
Range					
Test		3.16[1]	3.08[1]	2.56[1]	0.16[1]
			2.89[2]	2.77[2]	3.10[2]
P value		<0.001[1]	<0.001[1]	0.01[1]	0.87[1]
			0.006[2]	0.008[2]	<0.001[2]
5. Glutathione peroxidase (GPx) u/ml	101.28±12.38	42.75±4.57	61.43±6.01	82.35±12.47	99.12±12.65
Mean ±SD	88.5 – 117.5	36.9 – 48.7	55.8 – 70.4	63.2 – 97.4	80.8 – 114.3
Test		3.50[1]	2.70[1]	2.24[1]	0.32[1]
			2.51[2]	2.33[2]	3.11[2]
P value		<0.001[1]	0.009[1]	0.025[1]	0.75[1]
			0.01[2]	0.02[2]	<0.001[2]

1: Comparing with control. 2: Comparing with MNI-7 group.

in serum MDA levels compared with the MNI-7 group (P < 0.001), with non-significant difference when compared with the control group (P = 0.06) (Table I, Fig. 1).

Serum GSH, SOD, CAT, and GPx levels revealed a highly significant reduction in the MNI-7 group compared to the control group (P < 0.001). Compared with the MNI-7 group, these antioxidant parameters showed a significant increase in the MNI-28 and MNI & STG-7 groups (P values ranging from 0.006 to 0.037).

Despite partial recovery, the MNI-28 group still exhibited a significant reduce in GSH, SOD, and GPx levels and a highly significant reduction in CAT activity compared to the control group. The MNI & STG-7 group illustrated a significant decline in GSH, CAT, and GPx levels, whereas SOD activity did not substantially deviate from the control values.

In contrast, the MNI & STG-28 group demonstrated a highly significant increase in GSH, SOD, CAT, and GPx levels compared with the MNI-7 group (P < 0.001), with non-significant difference compared to the control group (Table I, Fig. 1).

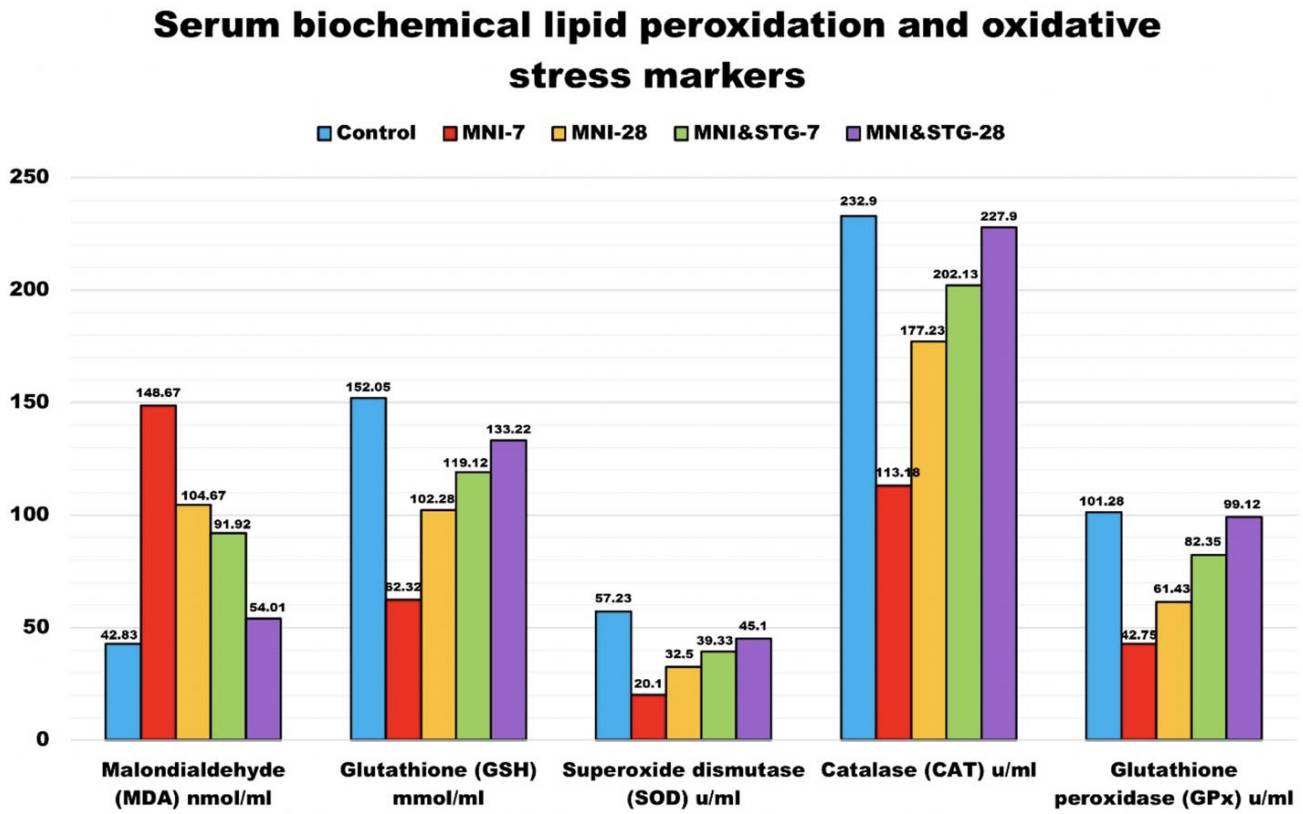

Fig. 1. Histogram of the serum biochemical lipid peroxidation and oxidative stress markers displaying a high significant elevation (P<0.001) of serum MDA in MNI-7, MNI-28 and MNI & STG-7 groups comparing to the control group, and a significant reduce in MNI-28 and MNI & STG-7 groups comparing to MNI-7 group. MNI & STG-28 group displaying a high significant reduction (P<0.001) in MDA level when comparing to MNI-7 and a non-significant variation (P=0.06) with the control group. Serum GSH, SOD, CAT, and GPx establishing a high significant decline (P<0.001) in MNI-7 group comparingto the control, and a significant improve in MNI-28 and MNI & STG-7 groups comparing to MNI-7 group. Moreover, GSH, SOD, and GPx levels demonstrating a significant decrease, and serum CAT revealing a high significant reduction (P<0.001) in MNI-28 group when comparing to the control. Additionally, serum GSH, CAT, and GPx illustrating a significant decrease, and serum SOD displaying a non-significant difference in MNI & STG-7 group comparing to the control group. Group MNI & STG-28 serum GSH, SOD, CAT, and GPx showing a marked significant rise (P<0.001) comparing to MNI-7 group with a non-significant difference comparing with the control group.

Serum inflammatory markers

Serum interleukin-6 (IL-6) levels showed a highly significant elevation in the MNI-7 and MNI-28 groups compared to the control group (P < 0.001). A significant increase was also noted in the MNI & STG-7 group compared to the control group (P = 0.04). Compared with the MNI-7 group, IL-6 levels were highly significantly reduced in the MNI-28, MNI & STG-7, and MNI & STG-28 groups (P < 0.001). In the MNI & STG-28 group, IL-6

levels showed no statistical significant difference when compared to the control group (P = 0.09) (Table II, Fig. 2).

Serum TNF-a levels were highly significantly elevated in the MNI-7 and MNI-28 groups compared to the control group (P < 0.001). The MNI & STG-7 group also showed a significant increase compared with the control group (P = 0.006). When compared with the MNI-7 group, TNF-a levels were significantly reduced in the MNI-28 and MNI & STG-7 groups. The MNI & STG-28 group demonstrated a highly significant decline compared with the MNI-7 group (P < 0.001), with no statistically significant difference compared with the control group (P = 0.06) (Table II, Fig. 2).

Table II. Serum biochemical inflammatory markers in the studied groups.

	Studied groups				
	Control	**MNI-7**	**MNI-28**	**MNI & STG-7**	**MNI & STG-28**
1. Interleukin 6 (IL-6) pg/ml	39.88±4.7	183.9±10.21	120.52±13.98	73.4±8.11	48.17±8.52
Mean ±SD	33.4 – 45.3	166.5 – 194	100 – 139.2	63.7 – 84.7	38.9 – 61.2
Range					
Test		3.17[1]	3.01[1]	2.26[1]	1.68[1]
			3.11[2]	3.88[2]	3.14[2]
P value		<0.001[1]	<0.001[1]	0.04[1]	0.09
			<0.001[2]	<0.001[2]	<0.001[2]
2. Tumor necrosis factor alpha (TNF-α) pg/ml	18.97±9.76	98.65±10.26	70.52±4.35	41.80±7.67	34.85±5.19
	9 – 35.6	86.5 – 111.4	65.7 – 77.4	31.5 – 54.8	24.7 – 39.6
Mean ±SD					
Range					
Test		4.21[1]	3.16[1]	2.72[1]	1.92[1]
			2.36[2]	2.80[2]	3.11[2]
P value		<0.001[1]	<0.001[1]	0.006[1]	0.06[1]
			0.03[2]	0.005[2]	<0.001[2]

1: Comparing with control. 2: Comparing with MNI-7 group.

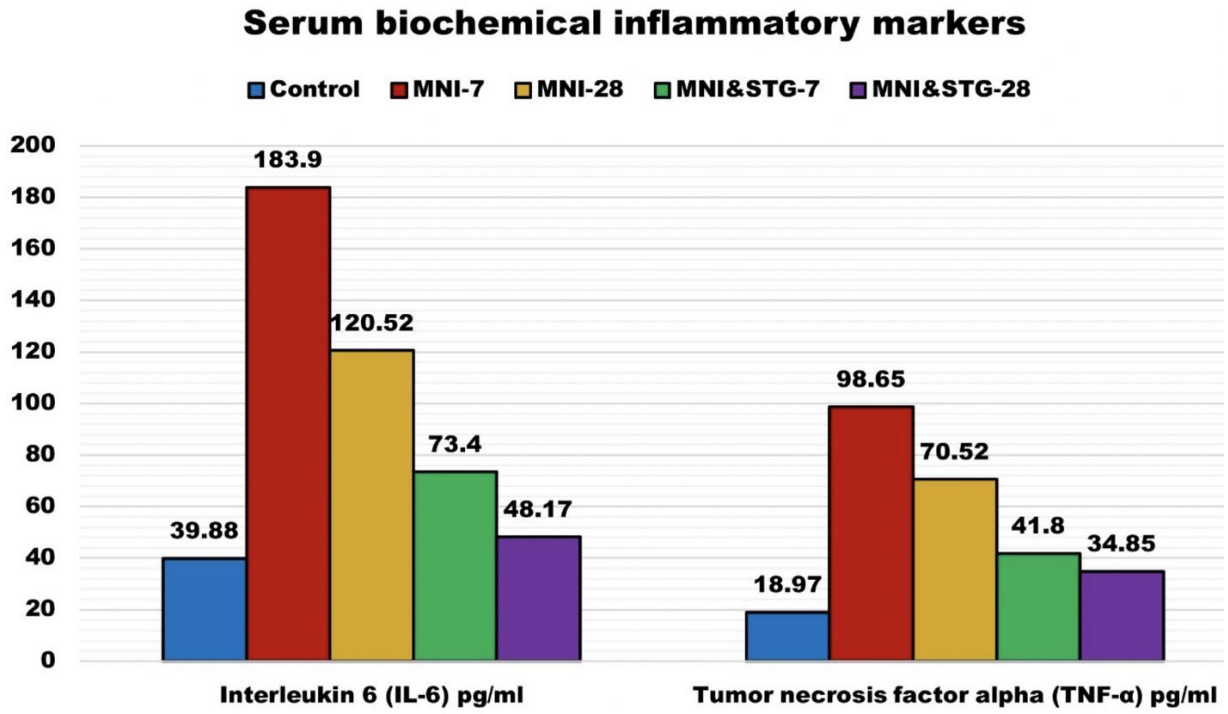

Fig. 2. Histogram of the serum biochemical inflammatory markers presenting a high significant increase (P<0.001) of IL-6 serum level in MNI-7, MNI-28 groups with a significant rise (P=0.04) in MNI & STG-7 group comparing to the control group. Controversy MNI-28, MNI & STG-7, and MNI & STG-28 groups illustrating a high significant reduction (P<0.001) comparing to MNI-7 group. However, MNI & STG-28 group showing a non-significant variation (P=0.09) with the control group. Serum TNF-a revealing a high significant rise (P<0.001) in MNI-7, MNI-28 groups and a significant increase (P=0.006) in MNI & STG-7 group comparing to the control group. In contrast MNI-28 and MNI & STG-7 groups illustrating a significant decrease comparing to MNI-7 group. But, TNF-a level in MNI & STG-28 group showing a high significant decline (P<0.001) comparing to MNI-7 group and a non-significant variation (P=0.06) than the control group.

Serum nerve growth factor (NGF)

Serum nerve growth factor (NGF) levels displayed a highly significant decline in the MNI-7 and MNI-28 groups compared with the control group (P < 0.001). A significant decrease was also noted in the MNI & STG-7 group compared with the control group (P = 0.008). When compared with the MNI-7 group, NGF levels showed a significant rise in the MNI-28 and MNI & STG-7 groups (P = 0.01 and P = 0.009, respectively). The MNI & STG-28 group demonstrated a significant increase compared with the MNI-7 group (P = 0.005), with no statistical significant difference compared to the control group (P = 0.07) (Table III, Fig. 3).

In contrast, groups MNI-28 and MNI & STG-7 displaying a significant rise when comparing to MNI-7 group. In MNI & STG-28 group, serum NGF showing a significant increase (P=0.005) in comparison to MNI-7 group and a non-significant decrease (P=0.07) when comparing to the control.

Table III. Serum biochemical nerve growth factor (NGF) marker in the studied groups.

	Studied groups				
	Control	**MNI-7**	**MNI-28**	**MNI & STG-7**	**MNI & STG-28**
Nerve growth factor (NGF) pg/ml Mean ±SD Range	216.53±9.44 199.2 – 225.6	155.85±11.32 142.3 – 170.5	178.28±9.11 165.4 – 189.7	185.67±9.11 173 – 199	206.37±10.32 192.3 – 220.3
Test		3.87[1]	2.98[1]	2.57[1]	1.85[1]
			2.56[2]	2.64[2]	2.84[2]
P value		<0.001[1]	<0.001[1]	0.008[1]	0.07[1]
			0.01[2]	0.009[2]	0.005[2]

1: Comparing with control. 2: Comparing with MNI-7 group.

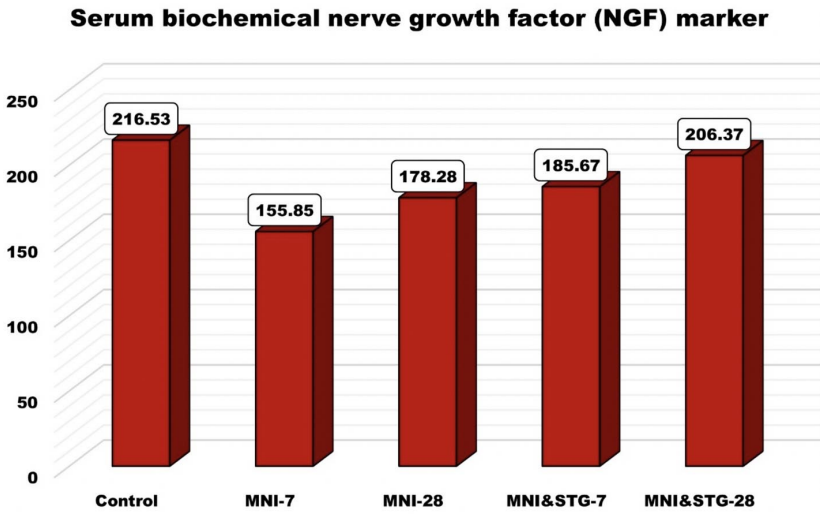

Fig. 3. Histogram of the serum biochemical NGF marker presenting a high significant decrease (P<0.001) of NGF in MNI-7, and MNI-28 groups, and a significant decline (P=0.008) in MNI & STG-7 group comparing to the control.

Histological, morphometrical, and statistical analysis results

Hematoxylin and eosin histological stain results

H&E–stained longitudinal sections of the median nerve from all studied groups were carefully examined. Sections from the control group demonstrated the typical histological architecture of the adult rat median nerve, characterized by closely packed, parallel myelinated nerve fibers with oval basophilic Schwann cell nuclei located between the fibers (Fig. 4A).

Sections from the MNI-7 group revealed severe histopathological alterations, including widely separated nerve fibers, multiple areas of vacuolation, marked nerve fiber loss, and discontinuity of nerve fibers. In addition, diffuse mononuclear inflammatory cell infiltration was observed, along with dilated and congested blood vessels (Figs. 4BI,BII).

The MNI-28 group exhibited minimal histological improvement, as nerve fibers remained separated with persistent areas of vacuolation and nerve fiber loss. Mononuclear inflammatory cell infiltration was still clearly evident (Fig. 4C).

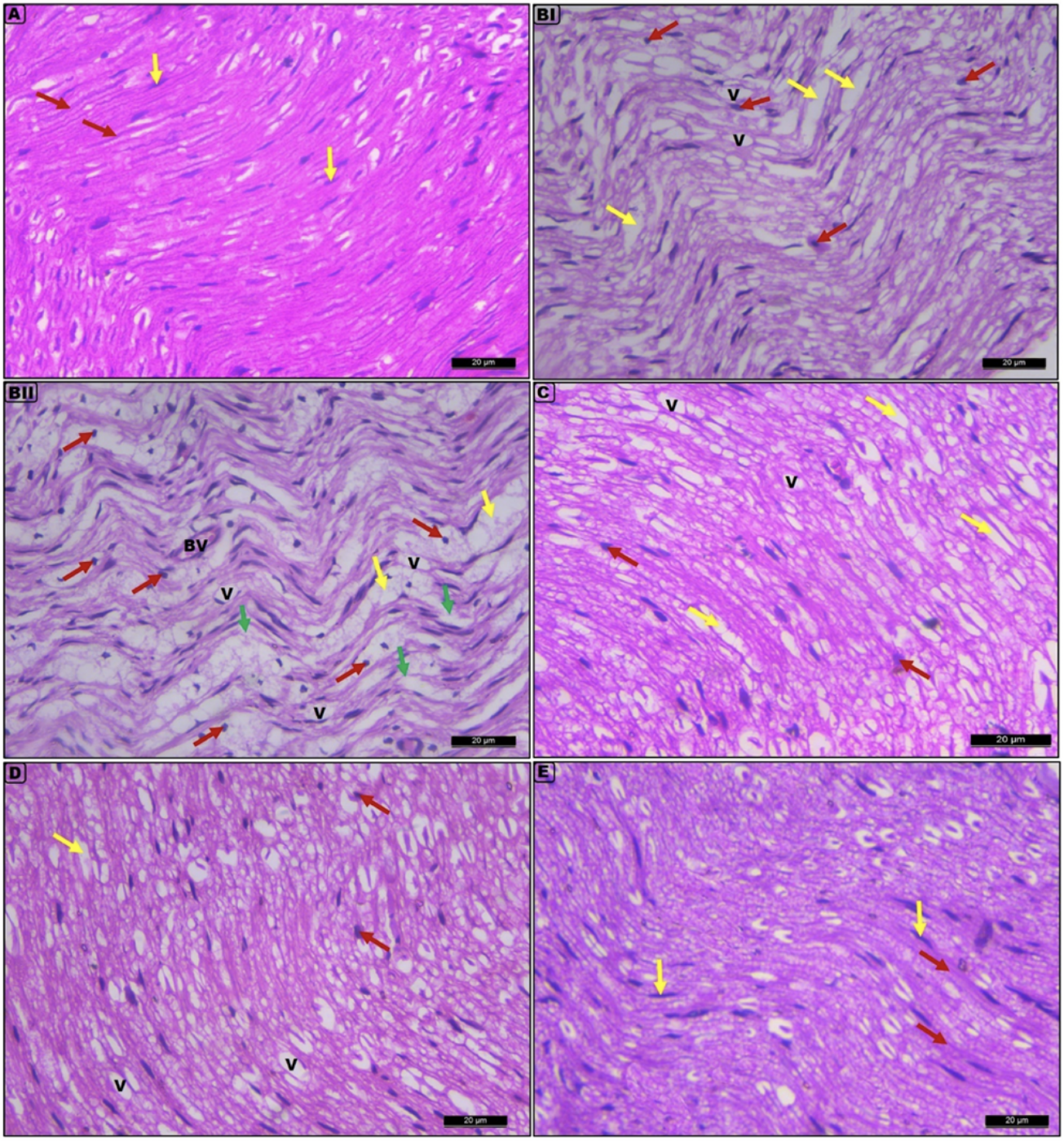

Fig. 4. H&E photomicrographs of longitudinal sections of median nerve (scale bar=20 µm, ×400) revealed: **A**. Control group of adult rat median nerve presenting normal architecture of rat's median nerve. There are notable parallel myelinated nerve fibers (red arrow), with oval basophilic Schwann cell nuclei (yellow arrow) between the fibers. BI. MNI-7 group displaying severe pathological changes in the form of widely separated nerve fibers with several vacuolated areas (V), nerve fiber loss (yellow arrow) and prominent mononuclear cell infiltration (red arrow). BII. MNI-7 group displaying the same severe pathological changes as BI photomicrograph in the form of widely separated nerve fibers with several vacuolated areas (V) and nerve fiber loss (yellow arrow). Additionally, there is discontinuity of nerve fibers (green arrow), and eminent spread of mononuclear cell infiltration (red arrow) with some dilated and congested blood vessels (BV) were also noted. **C.** MNI-28 group showing minimal improvement as the nerve fibers are still separated with many areas of vacuolation (V) and nerve fiber loss (yellow arrow). Also, obvious mononuclear cell infiltration (red arrow) is still present. **D.** MNI & STG-7 group: demonstrating improvement with minimal nerve fibers were still separated with areas of vacuolation (V) and nerve fiber loss (yellow arrow). Minimal mononuclear cell infiltration (red arrow) is still present. **E.** MNI & STG-28 group: showing restoration of normal architecture of rat's median nerve nearly resembling the control where there are parallel myelinated nerve fibers (red arrow), with oval basophilic Schwann cell nuclei (yellow arrow) between the fibers.

Sections from the MNI & STG-7 group showed partial improvement in nerve fiber arrangement; however, some nerve fibers were still separated, with residual areas of vacuolation and nerve fiber loss. Mononuclear inflammatory cell infiltration remained apparent (Fig. 4D).

In contrast, sections from the MNI & STG-28 group demonstrated a histological appearance closely resembling that of the control group, with restoration of the normal architecture of the rat median nerve and marked attenuation of the histological changes induced by the crush injury (Fig. 4E).

Masson's Trichrome histological stain results

Masson's trichrome-stained sections from the control group revealed regularly arranged collagen fibers. The MNI-7 group exhibited marked disorganization of collagen fibers with extensive areas of collagen loss. The MNI-28 group showed moderate collagen disorganization, while the MNI & STG-7 group displayed mild disruption. The MNI & STG-28 group showed collagen fiber organization comparable to the control group.

Morphometric analysis revealed a highly significant rise in the mean area percent of collagen fiber deposition in the MNI-7, MNI-28, and MNI & STG-7 groups compared to the control group ($P < 0.001$). When compared with the MNI-7 group, a significant reduction was observed in the MNI-28 and MNI & STG-7 groups. The MNI & STG-28 group demonstrated a highly significant decrease compared with the MNI-7 group ($P < 0.001$), with no statistical significant difference compared to the control group (Table IV, Fig. 5).

Table IV. Area percentage of collagen fiber deposition in the studied groups.

Area % of collagen fiber deposition	Studied groups				
	Control	MNI-7	MNI-28	MNI & STG-7	MNI & STG-28
Mean ±SD	9.50±1.87	118.83±25.24	88.83±12.87	70.0±15.30	12.33±4.88
Range	7 – 12	90 – 152	72 – 108	59 – 98	5 – 18
Test		3.53[1]	4.94[1]	3.61[1]	1.32[1]
			2.05[2]	3.01[2]	1.10[2]
P value		<0.001[1]	<0.001[1]	<0.001[1]	0.23[1]
			0.036[2]	0.001[2]	<0.001[2]

1: Comparing with control. 2: Comparing with MNI-7 group.

Immunohistochemical, Morphometrical, and Statistical analysis results

Glial fibrillary acidic protein (GFAP).

GFAP immunostaining was negative in the control group. The MNI-7 group showed a marked positive immunoreaction, while the MNI-28 group exhibited moderate positivity. Mild positivity was observed in the MNI & STG-7 group. The MNI & STG-28 group showed a negative immunoreaction comparable to the control group.

Morphometric analysis demonstrated a highly significant rise in GFAP immunoexpression in the MNI-7, MNI-28, and MNI & STG-7 groups compared to the control group ($P < 0.001$). Compared with the MNI-7 group, GFAP expression was significantly reduced in the MNI-28 and MNI & STG-7 groups. The MNI & STG-28 group illustrated a highly significant decline compared with the MNI-7 group, with no statistical significant difference compared with the control group (Table V, Fig. 6).

Nuclear factor erythroid 2-related factor 2 (Nrf2).

Nrf2 immunostaining showed a strong positive reaction in the control group. The MNI-7 group exhibited a markedly negative reaction, while the MNI-28 group showed mild positivity. Moderate immunoreactivity was observed in the MNI & STG-7 group. The MNI & STG-28 group demonstrated strong immunoreactivity comparable to the control group.

Morphometric analysis revealed a highly significant decrease in Nrf2 immunoexpression in the MNI-7 group compared to the control group ($P < 0.001$). Compared with the MNI-7 group, Nrf2 expression showed a significant rise in the MNI-28 and MNI & STG-7 groups. The MNI & STG-28 group demonstrated a highly significant increase compared with the MNI-7 group, with no statistically significant difference compared with the control group (Table V, Fig. 7).

BAX

BAX immunostaining was negative in the control group. The MNI-7 group exhibited a marked positive immunoreaction, while the MNI-28 group showed moderate positivity. Mild positivity was observed in the MNI & STG-7 group. The MNI & STG-28 group showed a negative immunoreaction comparable to the control group.

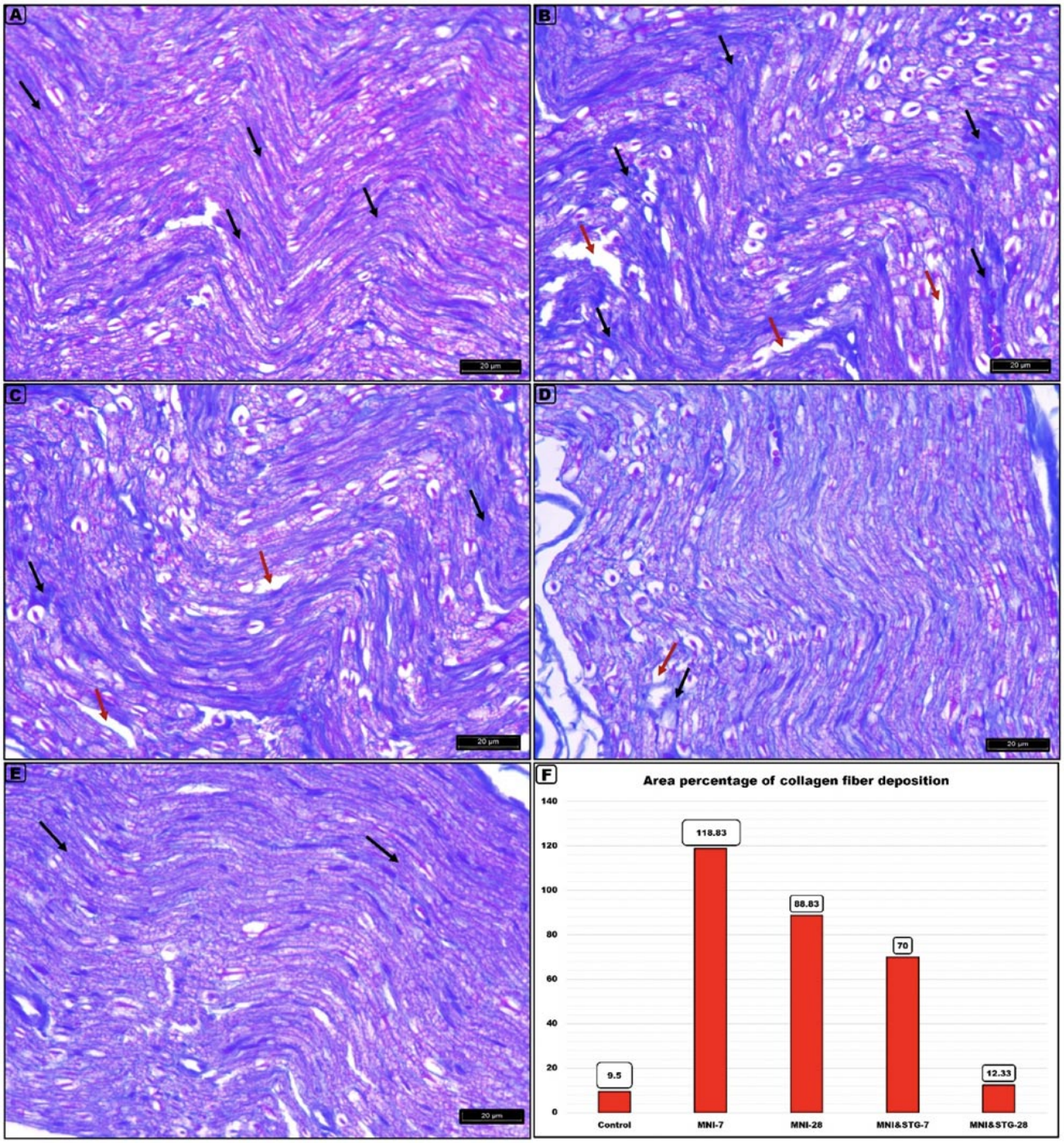

Fig. 5. Masson's Trichrome stain photomicrographs of longitudinal sections of median nerve revealed: **A.** Control group of adult rat median nerve revealing closely packed well-organized collagen fibers (black arrow). (scale bar=20 µm, ×400). **B.** MNI-7 group demonstrating disorganized collagen fibers (black arrow) with several spaces of collagen loss (red arrow). (scale bar=20 µm, ×400). **C.** MNI-28 group showing moderate disorganized collagen fibers (black arrow) with moderate spaces of collagen loss (red arrow). (scale bar=20 µm, ×400). **D.** MNI & STG-7 group: presenting minimal disorganized collagen fibers (black arrow) with minimal spaces of collagen loss (red arrow). (scale bar=20 µm, ×400). **E.** MNI & STG-28 group: revealing closely packed well-organized collagen fibers (black arrow) nearly similar to control. (scale bar=20 µm, ×400). **F.** Histogram of the mean area % of collagen fiber deposition displaying a noticeable high significant rise in MNI-7, MNI-28, and MNI & STG-7 groups ($P<0.001$) in comparison to the control group. However, there is a significant decline in both MNI-28 and MNI & STG-7 groups comparing to MNI-7 group. In MNI & STG-28 group, there is a noteworthy highly significant decrease ($P<0.001$) when comparing to MNI-7 group and non-significant increase ($P=0.23$) comparing to the control group.

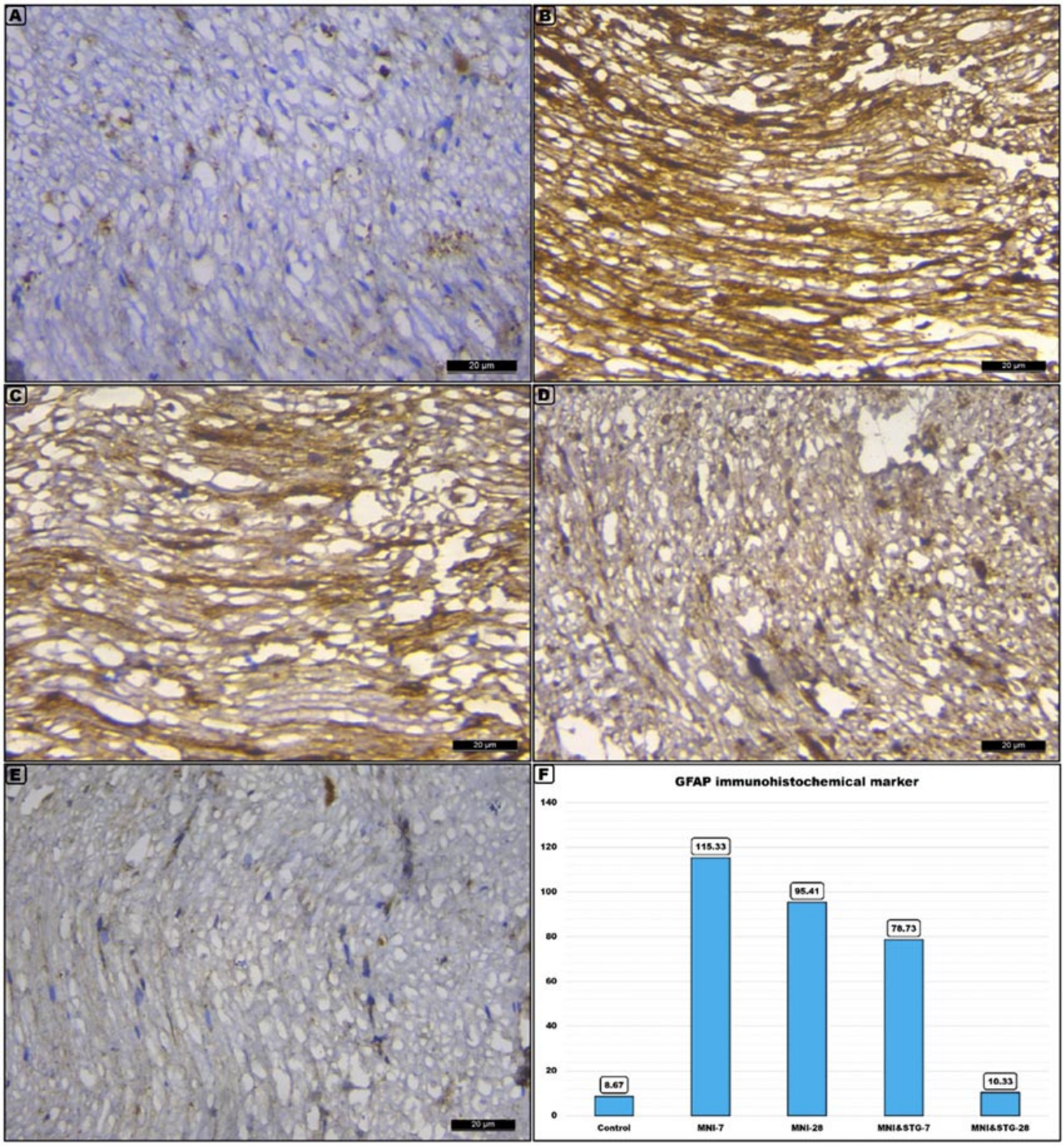

Fig. 6. GFAP immunostaining photomicrographs of longitudinal sections of median nerve demonstrated: **A.** Control group of adult rat median nerve displaying a negative GFAP immune reaction in Schwann cells of myelinated nerve axons. (scale bar=20 µm, ×400) **B.** MNI-7 group showing a remarkable marked positive GFAP immune reaction in Schwann cells of myelinated nerve axons. (scale bar=20 µm, ×400). **C.** MNI-28 group: illustrating moderate positive GFAP immune reaction in Schwann cells of myelinated nerve axons. (scale bar=20 µm, ×400). **D.** MNI & STG-7 group: revealing mild positive GFAP immune reaction in Schwann cells of myelinated nerve axons. (scale bar=20 µm, ×400). **E.** MNI & STG-28 group: demonstrating negative GFAP immune reaction in Schwann cells of myelinated nerve axons. (scale bar=20 µm, ×400). **F.** Histogram of the mean area % of GFAP immunostaining presenting a remarkable high significant increase in MNI-7, MNI-28, and MNI & STG-7 groups ($P<0.001$) comparing to the control group. Conversely, a significant decline in both MNI-28 and MNI & STG-7 groups comparing to MNI-7 group. There is also a notable high significant reduction ($P<0.001$) in MNI & STG-28 group when comparing to MNI-7 group and a non-significant variation ($P=0.57$) with the control group.

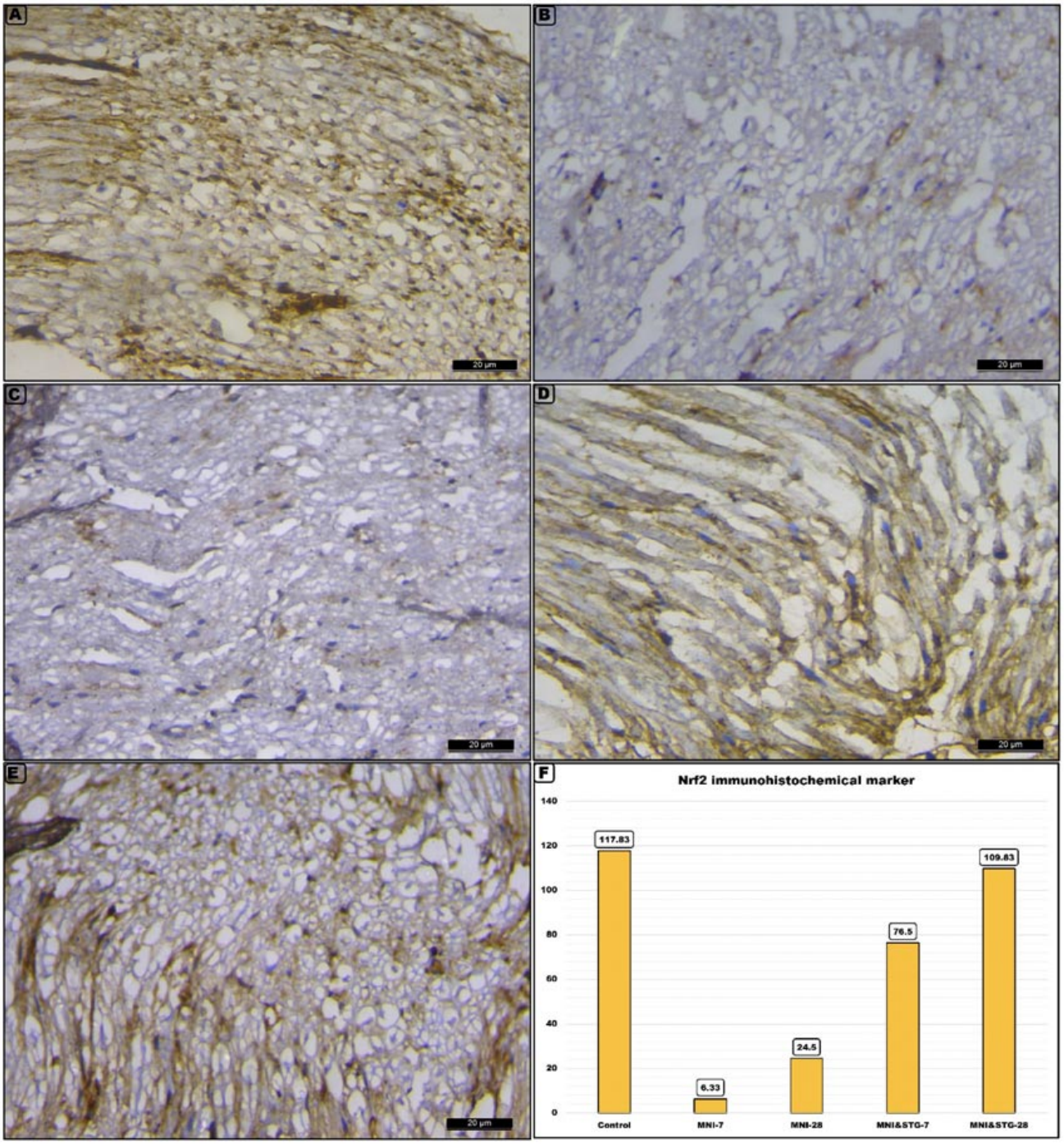

Fig. 7. Nrf2 immunostaining photomicrographs of longitudinal sections of median nerve demonstrated:
A. Control group of adult rat median nerve displaying marked positive reaction for Nrf2 immunostain. (scale bar=20 µm, ×400)
B. MNI-7 group showing a negative Nrf2 immune reaction. (scale bar=20 µm, ×400)
C. MNI-28 group: illustrating mild positive immune reaction for Nrf2. (scale bar=20 µm, ×400)
D. MNI & STG-7 group: revealing moderate positive immune reaction for Nrf2. (scale bar=20 µm, ×400)
E. MNI & STG-28 group: showing strong positive immune reaction for Nrf2. (scale bar=20 µm, ×400).
F. Histogram of the mean area % of Nrf2 immunostaining displaying a noticeable high significant decline in MNI-7 group when comparing to the control group ($P<0.001$). But, MNI-28 and MNI & STG-7 groups demonstrating a significant rise comparing to MNI-7 group. MNI & STG-28 group showing a high significant rise when comparing to MNI-7 group ($P<0.001$) and a non-significant variation with the control group.

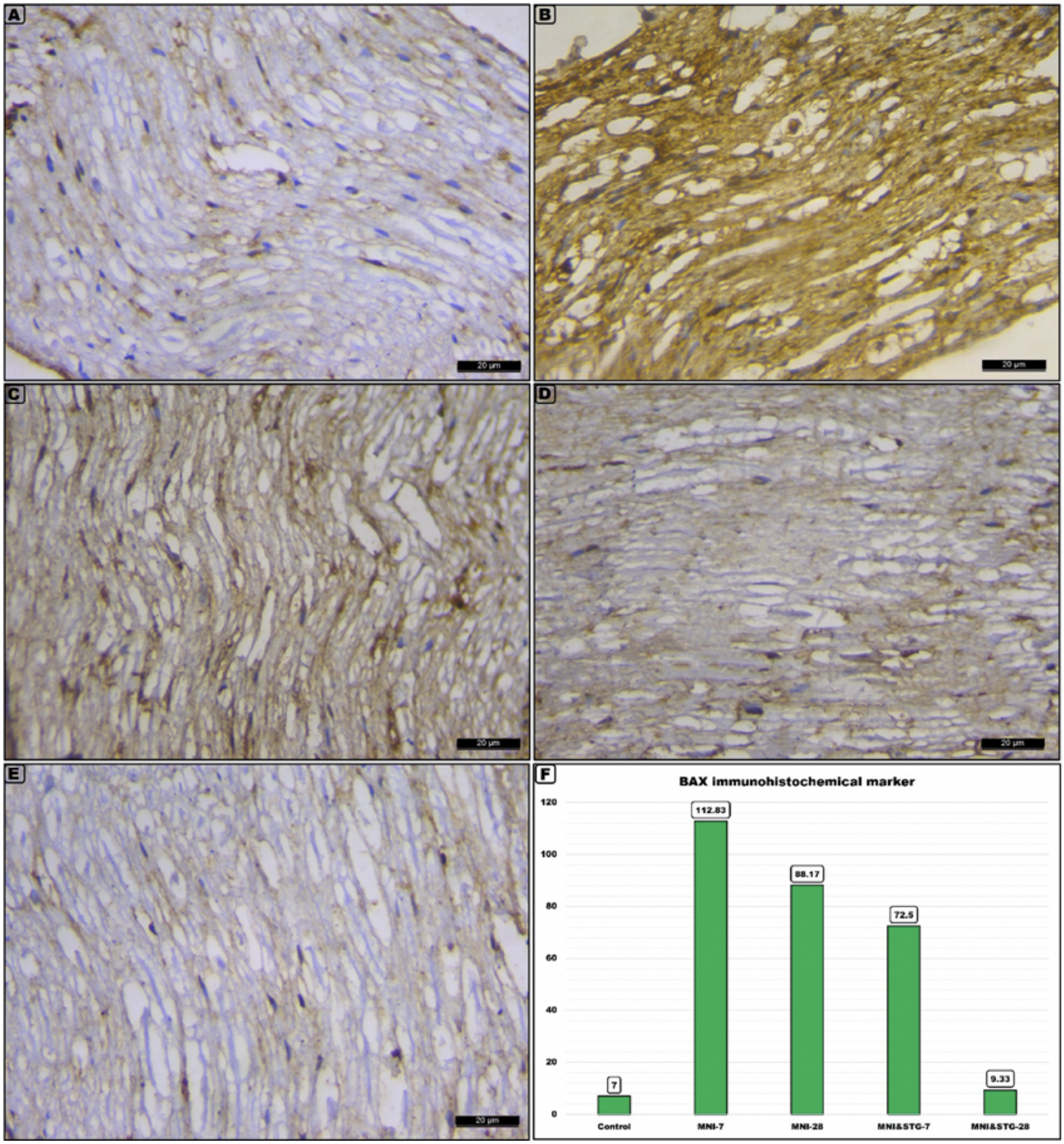

Fig. 8. BAX immunostaining photomicrographs of longitudinal sections of median nerve demonstrated:
A. Control group of adult rat median nerve displaying negative reaction for BAX immunostaining. (scale bar=20 µm, ×400)
B. MNI-7 group showing a marked positive immune reaction for BAX immunostaining. (scale bar=20 µm, ×400)
C. MNI-28 group: demonstrating a moderately positive reaction for BAX immunostaining. (scale bar=20 µm, ×400)
D. MNI & STG-7 group: revealing a mild positive reaction for BAX immunostaining. (scale bar=20 µm, ×400)
E. MNI & STG-28 group: showing negative reaction for BAX immunostaining. (scale bar=20 µm, ×400)
F. Histogram of the mean area % of BAX immunostaining demonstrating a notable high significant increase in MNI-7, MNI-28, and MNI & STG-7 groups ($P<0.001$) comparing to the control group. However, a significant decline in both MNI-28 and MNI & STG-7 groups comparing to MNI-7 group. MNI & STG-28 group illustrating a marked high significant decrease ($P<0.001$) comparing to MNI-7 group and a non-significant difference ($P=0.38$) when comparing to the control group.

Table V. Immunohistochemical markers in the studied groups.

	Studied groups				
	Control	**MNI-7**	**MNI-28**	**MNI & STG-7**	**MNI & STG-28**
1. GFAP					
Mean ±SD	8.67±3.44	115.33±5.39	95.41±15.75	78.73±8.93	10.33±5.43
Range	4 – 12	107 – 120	73 – 115	66 – 91	5 – 19
Test		5.12[1]	4.11[1]	3.83[1]	0.56[1]
			2.52[2]	2.89[2]	4.89[2]
P value		<0.001[1]	<0.001[1]	<0.001[1]	0.57[1]
			0.02[2]	0.004[2]	<0.001[2]
2. Nrf2					
Mean ±SD	117.83±5.71	6.33±2.94	24.50±7.81	76.50±10.54	109.83±10.11
Range	110 – 125	1 – 9	16 – 33	62 – 92	95 – 121
Test		6.13	5.89	2.64	1.36
			2.31	2.88	3.11
P value		<0.001[1]	<0.001[1]	0.01[1]	0.17[1]
			0.04[2]	0.004[2]	<0.001[2]
3. BAX					
Mean ±SD	7.0±4.19	112.83±12.89	88.17±13.21	72.5±14.4	9.33±4.37
Range	1 – 12	94 – 131	71 – 105	50 – 90	4 – 15
Test		5.16[1]	4.87[1]	4.12[1]	0.89[1]
			2.48[2]	2.88[2]	3.17[2]
P value		<0.001[1]	<0.001[1]	<0.001[1]	0.38[1]
			0.01[2]	0.004[2]	<0.001[2]

1: Comparing with control. 2: Comparing with MNI-7 group.

Morphometric analysis demonstrated a highly significant raise in BAX immunoexpression in the MNI-7, MNI-28, and MNI & STG-7 groups compared to the control group ($P < 0.001$). Compared with the MNI-7 group, BAX expression was reduced significantly in the MNI-28 and MNI & STG-7 groups. The MNI & STG-28 group demonstrated a highly significant lower compared with the MNI-7 group, with non-statistically significant difference compared with the control group (Table V, Fig. 8).

DISCUSSION

Peripheral nerve injury (PNI) represents a significant clinical challenge because of its heterogeneous etiology and variable severity, which may result in outcomes ranging from mild functional impairment to complete loss of motor and sensory function (Patel *et al*., 2018). In addition, PNI induces molecular and cellular alterations that contribute to progressive muscle atrophy and dysfunction, particularly in chronic or untreated cases (Yadav & Dabur, 2024). Despite advances in microsurgical techniques and improvements in rehabilitative care, optimal functional recovery of injured peripheral nerves remains unsatisfactory (Somay *et al*., 2017).

Among the different mechanisms of peripheral nerve injury, crush injury is one of the most frequently encountered and experimentally reproducible models (Alvites *et al*., 2018). Accordingly, a crush injury model was selected in the present study to investigate the pathological changes following median nerve injury and to evaluate the potential neuroregenerative effects of STG.

As part of drug repositioning strategies, DPP-4 inhibitors such as STG have attracted increasing attention for their potential therapeutic applications beyond glycemic control (Pushpakom *et al*., 2019). Several studies have displayed that DPP-4 inhibitors possess neuroprotective properties capable of attenuating neuronal degeneration and improving neural tissue integrity (Abdelsalam & Safar, 2015). Therefore, the present study sought to assess the neuroregenerative potential of STG in a rat model of median nerve crush injury using biochemical, histological, immunohistochemical, and morphometric approaches.

In the present study, the MNI-7 group demonstrated a marked increase in serum MDA levels, reflecting enhanced lipid peroxidation and oxidative stress following nerve injury. These results align with earlier studies indicating early activation of lipid peroxidation after peripheral nerve damage, with MDA serving as a sensitive biomarker of oxidative injury and demyelination (Kongsui *et al*., 2023). Concomitantly, the significant reduction in endogenous antioxidant enzymes, including GSH, SOD, CAT, and GPx, further confirms the presence of pronounced oxidative stress in crushed median nerves, as previously reported by Ogut *et al*. (2020). This oxidative imbalance has been attributed to excessive reactive oxygen species (ROS) generation following nerve injury, which accelerates neuronal degeneration and impairs regeneration (Kobayashi *et al*., 2012).

ROS are known to promote lipid peroxidation and disrupt antioxidant defense systems, ultimately triggering necrotic or apoptotic cell death (Ragy, 2015). This

mechanism was supported in the present study by the marked increase in BAX immunoexpression in the MNI-7 group, indicating activation of pro-apoptotic pathways following nerve injury.

In addition to oxidative stress, inflammation plays a critical role in the progression of peripheral nerve damage. The present findings demonstrated significant elevations in inflammatory markers, IL-6 and TNF-a, in the early phase following median nerve injury. These results are consistent with previous studies reporting enhanced expression of pro-inflammatory mediators at the injury site, driven by activated Schwann cells and infiltrating macrophages, which further amplify oxidative stress and tissue damage (West *et al*., 2011; Yu *et al*., 2023).

Conversely, NGF levels were significantly decreased in the MNI-7 group. This observation aligns with previous findings showing diminished NGF expression in Schwann cells following peripheral nerve damage (Tosyalı *et al*., 2023). NGF plays a crucial role in the development, maintenance, and survival of sensory and sympathetic neurons, and its deficiency has been associated with impaired axonal growth and neuronal degeneration (Yamakita *et al*., 2017). Furthermore, NGF has been shown to enhance nerve regeneration and accelerate axonal elongation, highlighting its therapeutic relevance in peripheral nerve repair (Klein *et al*., 2022). The observed increase in NGF levels in the MNI-28, MNI & STG-7, and MNI & STG-28 groups suggest a gradual recovery process that is enhanced by sitagliptin treatment.

Histologically, the MNI-7 group exhibited severe structural alterations, including nerve fiber separation, vacuolation, fiber loss, increased collagen deposition, and inflammatory infiltration. Similar pathological features have been described in previous studies during the early phase following crush nerve injury (Ramli *et al*., 2017; Türedi *et al*., 2018). These changes are characteristic of Wallerian degeneration, which typically initiates within the first week after injury and peaks between days 3 and 7, facilitating debris clearance but also contributing to transient functional deterioration (Wang *et al*., 2018). Increased vascular permeability and endoneurial edema further exacerbate ischemia and oxidative damage, leading to axonal degeneration and myelin breakdown (Gao *et al*., 2013).

Immunohistochemical analysis in the current study revealed a marked raise in GFAP expression following median nerve injury, reflecting Schwann cell activation and reactive gliosis. Similar increases in GFAP expression have been reported following peripheral nerve crush injury and are indicative of Schwann cell proliferation and dedifferentiation during early regenerative responses (Gugliandolo *et al*., 2018). GFAP plays an essential role in Schwann cell plasticity and axonal regeneration, and its absence has been associated with delayed nerve repair (Triolo *et al*., 2006; Berg *et al*., 2013).

In contrast, Nrf2 immunoexpression was significantly reduced following nerve injury, consistent with previous reports demonstrating impaired antioxidant defense mechanisms after peripheral nerve damage (Tosyalı *et al*., 2023). Nrf2 is a key transcription factor regulating cellular antioxidant responses, and its suppression contributes to increased vulnerability to oxidative stress (Oh & Jun, 2017). Reduced Nrf2 activity has also been associated with metabolic stress conditions, including diabetes, which further compromise antioxidant capacity (Tan *et al*., 2011).

Treatment with STG resulted in marked improvement across all evaluated parameters. Sitagliptin administration significantly reduced oxidative stress markers while restoring antioxidant enzyme activity, consistent with previous studies demonstrating its potent antioxidant and free radical scavenging properties (Pintana *et al*., 2013; Jamwal & Kumar, 2019; Kabel *et al*., 2019). In addition, sitagliptin enhanced NGF levels and improved histological organization of nerve fibers, supporting its role in promoting neuroregeneration and neuronal plasticity (Pansri *et al*., 2021).

The anti-inflammatory impacts of STG were further evidenced by the attenuation in IL-6 and TNF-a levels, in agreement with reports demonstrating that DPP-4 inhibitors modulate innate immune responses and suppress pro-inflammatory cytokine production (Zhong *et al*., 2013; Wicin´ski *et al*., 2018). Moreover, STG attenuated collagen deposition and fibrosis, consistent with findings in other tissues showing reduced extracellular matrix accumulation following sitagliptin supplementation (Alam *et al*., 2015). STG treatment also resulted in decreased GFAP expression, suggesting reduced glial activation and inflammation, consistent with previous studies linking GFAP reduction to improved neural outcomes (Sun *et al*., 2017; Song *et al*., 2024). Furthermore, enhanced Nrf2 expression in STG-treated groups supports activation of antioxidant signaling pathways, as previously demonstrated in renal and metabolic disease models (Wang *et al*., 2019; Kong *et al*., 2021; Abd-Eldayem *et al*., 2024). The activation of Nrf2-dependent pathways plays a crucial role in cellular defense against oxidative damage and regulation of inflammatory responses (He *et al*., 2020; Baird & Yamamoto, 2020).

Finally, STG significantly reduced BAX immunoexpression, indicating suppression of apoptosis.

Similar anti-apoptotic effects of STG have been reported in renal and neural tissues and are ascribed to its cytoprotective and antioxidant qualities (Abuelezz *et al*., 2016; Kizilay *et al*., 2021). Notably, prolonged STG treatment (MNI & STG-28 group) resulted in more pronounced improvements compared with shorter treatment duration, highlighting the importance of sustained therapy for optimal neuroregenerative outcomes.

CONCLUSIONS

Based on the findings of the current study, STG demonstrated a clear neuroregenerative effect following median nerve crush injury. This effect appears to be mediated, at least in part, through modulation of biochemical disturbances related to lipid peroxidation, oxidative stress, and inflammatory responses. In addition, STG markedly improved histopathological alterations of the injured median nerve, with enhanced restoration of nerve architecture, reduced glial activation and apoptosis, as evidenced by decreased GFAP and BAX immunoreactivity, and upregulation of the antioxidant regulator Nrf2.

The present results also support the concept that peripheral nerves possess an intrinsic capacity for spontaneous regeneration when an adequate recovery period is allowed, as reflected by the partial improvement observed in the median nerve injury 28-day group. However, recovery in the absence of pharmacological intervention remained incomplete when compared with STG-treated groups.
Taken together, these results suggest that STG may represent a recommended adjunctive therapeutic agent for enhancing peripheral nerve regeneration. Nevertheless, further experimental and clinical studies are warranted to evaluate different dosing regimens, treatment durations, and long-term functional outcomes in order to establish its potential clinical applicability.

SALAMA, R. M. & ZEDAN, O .I. Impacto neurorregenerativo del inhibidor de la dipeptidil peptidasa IV (sitagliptina) en la lesión del nervio mediano en ratas: Metodología bioquímica, histológica e inmunohistoquímica. *Int. J. Morphol., 44(1)*:258-275, 2026.

RESUMEN: La lesión del nervio periférico se asocia frecuentemente con una recuperación funcional incompleta a pesar de la intervención quirúrgica. La sitagliptina, un inhibidor de la dipeptidil peptidasa-4, ha demostrado propiedades anti-inflamatorias, antioxidantes y antiapoptóticas en diversos modelos animales. Este estudio se diseñó para evaluar el posible efecto neurorregenerativo de la sitagliptina tras una lesión por aplastamiento del nervio mediano en ratas. Cuarenta y ocho ratas albinas macho adultas fueron asignadas aleatoriamente a ocho grupos, incluyendo grupos de cirugía simulada, grupos tratados con sitagliptina, grupos con lesión del nervio mediano y grupos con lesión del nervio mediano tratados con sitagliptina, evaluados a los 7 y 28 días. La sitagliptina se administró por vía oral a una dosis de 10 mg/kg/día. La evaluación bioquímica incluyó marcadores de estrés oxidativo, enzimas antioxidantes, citocinas inflamatorias y factor de crecimiento nervioso. Se utilizaron hematoxilina y eosina y tricrómico de Masson para la evaluación histológica, mientras que el análisis inmunohistoquímico evaluó la expresión de GFAP, Nrf2 y BAX. La lesión por aplastamiento del nervio mediano a los 7 días (grupo MNI-7) resultó en estrés oxidativo marcado, respuesta inflamatoria, apoptosis, disrupción nerviosa estructural y deposición de colágeno, acompañados de niveles reducidos de factor de crecimiento nervioso. Mientras que el grupo MNI 28 ilustró inequívocamente cierta mejoría en todos los parámetros medidos. El tratamiento con sitagliptina atenuó significativamente la peroxidación lipídica, restauró la actividad enzimática antioxidante, redujo los marcadores inflamatorios y aumentó los niveles del factor de crecimiento nervioso. Los hallazgos histológicos e inmunohistoquímicos demostraron una mejor arquitectura nerviosa, una menor fibrosis, una menor inmunorreactividad de GFAP y BAX, y un aumento de la expresión de Nrf2, especialmente con el tratamiento prolongado. Estos hallazgos indican que la sitagliptina promueve la recuperación bioquímica y estructural tras una lesión por aplastamiento del nervio mediano, probablemente gracias a sus propiedades anti-inflamatorias, antioxidantes y antiapoptóticas, lo que apunta a un posible uso medicinal para promover la regeneración de los nervios periféricos.

PALABRAS CLAVE: Lesión de nervios periféricos; Sitagliptina; Estrés oxidativo; GFAP; Nrf2; BAX.

REFERENCES

Abd-Eldayem, A. M.; Makram, S. M.; Messiha, B. A. S.; Abd-Elhafeez, H. H. & Abdel-Reheim, M. A. Cyclosporine-induced kidney damage was halted by sitagliptin and hesperidin via increasing Nrf2 and suppressing TNF-α, NF-κB, and Bax. *Sci. Rep., 14(1)*:7434, 2024.

Abdelsalam, R. M. & Safar, M. M. Neuroprotective effects of vildagliptin in rat rotenone Parkinson's disease model: role of RAGE-NFkB and Nrf2-antioxidant signaling pathways. *J. Neurochem., 133(5)*:700-7, 2015.

Abuelezz, S. A.; Hendawy, N. & Abdel Gawad, S. Alleviation of renal mitochondrial dysfunction and apoptosis underlies the protective effect of sitagliptin in gentamicin-induced nephrotoxicity. *J. Pharm. Pharmacol., 68(4)*:523-32, 2016.

Alam, M. A.; Chowdhury, M. R. H.; Jain, P.; Sagor, M. A. T. & Reza, H. M. DPP-4 inhibitor sitagliptin prevents inflammation and oxidative stress of heart and kidney in two kidney and one clip (2K1C) rats. *Diabetol. Metab. Syndr., 7*:107, 2015.

Alvites, R.; Caseiro, A. R.; Pedrosa, S. S.; Branquinho, M. V.; Ronchi, G.; Geuna, S.; Varejão, A. S. P. & Maurício A. C. Peripheral nerve injury and axonotmesis: State of the art and recent advances. *Cogent. Med., 5(1)*:1-45, 2018.

Baird, L. & Yamamoto, M. The Molecular Mechanisms Regulating the KEAP1-NRF2 Pathway. *Mol. Cell Biol., 40(13)*:e00099-20, 2020.

Bancroft, J. D. & Gamble, M. *Theory and Practice of Histological Techniques*. 6th ed. Philadelphia, Churchill Livingstone, Elsevier, 2008. pp.126, 150, 440

Bassendine, M. F.; Bridge, S. H.; McCaughan, G. W. & Gorrell M. D. COVID-19 and comorbidities: A role for dipeptidyl peptidase 4 (DPP4) in disease severity? *J. Diabetes, 12(9)*:649-58, 2020.

Berg, A.; Zelano, J.; Pekna, M.; Wilhelmsson, U.; Pekny M. & Cullheim S. Axonal regeneration after sciatic nerve lesion is delayed but complete in GFAP- and vimentin-deficient mice. *PLoS One, 8(11)*:e79395, 2013.

Caillaud, M.; Richard, L.; Vallat, J.; Desmoulière, A. & Billet F. Peripheral nerve regeneration and intraneural revascularization. *Neural. Regen. Res., 14(1)*:24-33, 2019.

Ezzeddini, R.; Taghikhani, M.; Somi, M. H.; Samadi, N. & Rasaee, M. J. Clinical importance of FASN in relation to HIF-1a and SREBP-1c in gastric adenocarcinoma. *Life Sci., 224*:169-76, 2019.

Farahani, F. K.; Fattahian, H.; Asghari, A. & Mortazavi, P. The comparative effects of estrogen and tacrolimus on crushed sciatic nerve regeneration in male mice: functional and histopathological evaluation. *Vet. Res. Forum, 13(2)*:241-7, 2022.

Faroni, A.; Mobasseri, S. A.; Kingham, P. J. & Reid, A. J. Peripheral nerve regeneration: experimental strategies and future perspectives. *Adv. Drug Deliv. Rev., 82-83*:160-7, 2015.

Gao, Y.; Weng, C. & Wang, X. Changes in nerve microcirculation following peripheral nerve compression. *Neural. Regen. Res., 8(11)*:1041-7, 2013.

Gugliandolo, E.; D'amico, R.; Cordaro, M.; Fusco, R.; Siracusa, R.; Crupi, R.; Impellizzeri, D.; Cuzzocrea, S. & Di Paola, R. Effect of PEA-OXA on neuropathic pain and functional recovery after sciatic nerve crush. *J. Neuroinflammation, 15(1)*:264, 2018.

He, F.; Ru, X. & Wen, T. NRF2, a transcription factor for stress response and beyond. *Int. J. Mol. Sci., 21(13)*:4777, 2020.

Houschyar, K. S.; Momeni, A.; Pyles, M. N.; Cha, J. Y.; Maan, Z. N.; Duscher, D.; Jew, O. S.; Siemers, F. & van Schoonhoven, J. The role of current techniques and concepts in peripheral nerve repair. *Plast. Surg. Int., 2016*:4175293, 2016.

Huang, S.; Huang, Y.; Lin, W.; Wang, L.; Yang, Y.; Li, P.; Xiao, L.; Chen, Y.; Chu, Q. & Yuan X. Sitagliptin alleviates radiation-induced intestinal injury by activating NRF2-antioxidant axis, mitigating NLRP3 inf--lammasome activation, and reversing gut microbiota disorder. *Oxid. Med. Cell Longev., 2022*:2586305, 2022.

Jamwal, S. & Kumar, P. Insight into the emerging role of striatal neurotransmitters in the pathophysiology of Parkinson's disease and Huntington's disease: A review. *Curr. Neuropharmacol., 17(2)*:165-75, 2019.

Kabel, A.; Borg, H.; Abd Elmaaboud, M. & Ashour A. Ameliorative potential of sitagliptin and/or calcipotriol on lipopolysaccharide-induced Alzheimer's disease. *Bull. Egypt. Soc.Physiol. Sci., 39(2)*:191-203, 2019.

Karagiannis, T.; Boura, P. & Tsapas, A. Safety of dipeptidyl peptidase 4 inhibitors: A perspective review. *Ter. Adv. Drug Saf., 5(3)*:138-46, 2014.

Kizilay, G.; Ersoy, O.; Cerkezkayabekir, A. & Topcu-Tarladacalisir Y. Sitagliptin and fucoidan prevent apoptosis and reducing ER stress in diabetic rat testes. *Andrologia, 53(3)*:e13858, 2021.

Klein, S.; Siegmund, A.; Eigenberger, A.; Hartmann, V.; Langewost, F.; Hammer, N.; Anker, A.; Klein, K.; Morsczeck, C.; Prantl, L.; *et al*. Peripheral nerve regeneration-adipose-tissue-derived stem cells differentiated by a three-step protocol promote neurite elongation via NGF secretion. *Cells, 11(18)*:2887, 2022.

Kobayashi, M.; Ishibashi, S.; Tomimitsu, H.; Yokota, T. & Mizusawa, H. Proliferating immature Schwann cells contribute to nerve regeneration after ischemic peripheral nerve injury. *J. Neuropathol. Exp. Neurol., 71(6)*:511-9, 2012.

Kong, L.; Deng, J.; Zhou, X.; Cai, B.; Zhang, B.; Chen, X.; Chen, Z. & Wang, W. Sitagliptin activates the p62-Keap1-Nrf2 signalling pathway to alleviate oxidative stress and excessive autophagy in severe acute pancreatitis-related acute lung injury. *Cell Death Dis., 12(10)*:928, 2021.

Kongsui, R.; Surapinit, S.; Promsrisuk, T. & Thongrong, S. Pinostrobin from Boesenbergia rotunda attenuates oxidative stress and promotes functional recovery in rat model of sciatic nerve crush injury. *Braz. J. Med. Biol. Res., 56*:e12578, 2023.

Li, L.; Li, Y.; Fan, Z.; Wang, X.; Li, Z.; Wen, J.; Deng, J.; Tan, D.; Pan, M.; Hu, X.; *et al*. Ascorbic acid facilitates neural regeneration after sciatic nerve crush injury. *Front. Cell Neurosci., 13*:108, 2019.

Nemzek, J. A.; Bolgos, G. L.; Williams, B. A. & Remick, D. G. Differences in normal values for murine white blood cell counts and other hematological parameters based on sampling site. *Inflamm. Res., 50(10)*:523-7, 2001.

Ogut, E.; Yildirim, F. B.; Sarikcioglu, L.; Aydin, M. A. & Demir, N. Neuroprotective effects of ozone therapy after sciatic nerve cut injury. *Kurume Med. J., 65(4)*:137-44, 2020.

Oh, Y. S. & Jun, H. S. Effects of Glucagon-like peptide-1 on oxidative stress and Nrf2 signaling. *Int. J. Mol. Sci., 19(1)*:26, 2017.

Pansri, P.; Phanthong, P.; Suthprasertporn, N.; Kitiyanant, Y.; Tubsuwan, A. & Dinnyes, A. Brain-derived neurotrophic factor increases cell number of neural progenitor cells derived from human induced pluripotent stem cells. *PeerJ., 9*:e11388, 2021.

Patel, N. P.; Lyon, K. A. & Huang, J. H. An update-tissue engineered nerve grafts for the repair of peripheral nerve injuries. *Neural. Regen. Res., 13(5)*:764-74, 2018.

Pintana, H.; Apaijai, N.; Chattipakorn, N. & Chattipakorn, S. C. DPP-4 inhibitors improve cognition and brain mitochondrial function of insulin-resistant rats. *J. Endocrinol., 218(1)*:1-11, 2013.

Pushpakom, S.; Iorio, F.; Eyers, P. A.; Escott, K. J.; Hopper, S.; Wells, A.; Doig, A.; Guilliams, T.; Latimer, J.; McNamee, C.; *et al*. Drug repurposing: progress, challenges and recommendations. *Nat. Rev. Drug Discov., 18(1)*:41-58, 2019.

Ragy, M. M. Effect of exposure and withdrawal of 900-MHz-electromagnetic waves on brain, kidney and liver oxidative stress and some biochemical parameters in male rats. *Electromagn. Biol. Med., 34(4)*:279-84, 2015.

Ramli, D.; Aziz, I.; Mohamad, M.; Abdulahi, D. & Sanusi, J. The changes in rats with sciatic nerve crush injury supplemented with evening primrose oil: behavioural, morphologic, and morphometric analysis. *Evid. Based Complement Alternat. Med., 2017*:3476407, 2017.

Santos, A. P.; Suaid, C. A.; Xavier, M. & Yamane F. Functional and morphometric differences between the early and delayed use of phototherapy in crushed median nerves of rats. *Lasers Med. Sci., 27(2)*:479-86, 2012.

Somay, H.; Emon, S. T.; Uslu, S.; Orakdogen, M.; Meric, Z. C.; Ince, U. & Hakan, T. The histological effects of ozone therapy on sciatic nerve crush injury in rats. *World Neurosurg., 105*:702-8, 2017.

Song, J.; Li, M.; Kang, N.; Jin, W.; Xiao, Y.; Li, Z.; Qi, Q.; Zhang, J.; Duan, Y.; Feng, X. & Lv, P. Baicalein ameliorates cognitive impairment of vascular dementia rats via suppressing neuroinflammation and regulating intestinal microbiota. *Brain Res. Bull., 208*:110888, 2024.

Sun, Q.; Zhang, Y.; Huang, J.; Yu, F.; Xu, J.; Peng, B.; Liu, W.; Han, S.; Yin, J. & He, X. DPP4 regulates the inflammatory response in a rat model of febrile seizures. *Biomed. Mater Eng., 28(s1)*:S139-S152, 2017.

Suvarna, S. K.; Layton, C. & Bancroft, J. D. *Bancroft's Theory and Practice ff Histological Techniques.* 8th ed. London, Elsevier, 2019. pp.337-94.

Tan, Y.; Ichikawa, T.; Li, J.; Si, Q.; Yang, H.; Chen, X.; Goldblatt, C. S.; Meyer, C. J.; Li, X.; Cai, L.; *et al*. Diabetic downregulation of Nrf2 activity via ERK contributes to oxidative stress–induced insulin resistance in cardiac cells in vitro and in vivo. *Diabetes, 60(2)*:625-33, 2011.

Tosyalı, H. K.; Bora, E. S.; Çinarog˘lu, O. S. & Erbas¸, O. Oxytocin mitigates peripheral nerve damage via Nrf2 and irisin pathway. *Eur. Rev. Med. Pharmacol. Sci., 27(23)*:11340-50, 2023.

Triolo, D.; Dina, G.; Lorenzetti, I.; Malaguti, M.; Morana, P.; Del Carro, U.; Comi, G.; Messing, A.; Quattrini, A. & Previtali, S. C. Loss of glial fibrillary acidic protein (GFAP) impairs Schwann cell proliferation and delays nerve regeneration after damage. *J. Cell Sci., 119(19)*:3981-93, 2006.

Türedi, S.; Yulug, E.; Alver, A.; Bodur, A. & Ince, I. A morphological and biochemical evaluation of the effects of quercetin on experimental sciatic nerve damage in rats. *Exp. Ther. Med., 15(4)*:3215-24, 2018.

Wang, J.; Hu, L.; Chen, Y.; Fu, T.; Jiang, T.; Jiang, A. & You, X. Sitagliptin improves renal function in diabetic nephropathy in male Sprague Dawley rats through upregulating heme oxygenase-1 expression. *Endocrine, 63(1)*:70-8, 2019.

Wang, T.; Ito, A.; Aoyama, T.; Nakahara, R.; Nakahata, A.; Ji. X.; Zhang, J.; Kawai, H. & Kuroki, H. Functional evaluation outcomes correlate with histomorphometric changes in the rat sciatic nerve crush injury model: A comparison between sciatic functional index and kinematic analysis. *PLoS One, 13(12)*:e0208985, 2018.

West, A. P.; Shadel, G. S. & Ghosh, S. Mitochondria in innate immune responses. *Nat. Rev. Immunol., 11(6)*:389-402, 2011.

Wicinski, M.; Wódkiewicz, E.; Slupski, M.; Walczak, M.; Socha, M.; Malinowski, B. & Pawlak-Osinska, K. Neuroprotective activity of sitagliptin via reduction of neuroinflammation beyond the incretin effect: focus on Alzheimer's disease. *Biomed Res. Int., 2018(1)*: 6091014, 2018.

Yadav, A. & Dabur, R. Skeletal muscle atrophy after sciatic nerve damage: Mechanistic insights. *Eur. J. Pharmacol., 970*:176506, 2024.

Yamakita, S.; Matsuda, M.; Yamaguchi, Y.; Sawa, T. & Amaya, F. Dexmedetomidine prolongs levobupivacaine analgesia via inhibition of inflammation and p38 MAPK phosphorylation in rat dorsal root ganglion. *Neuroscience, 361*:58-68, 2017.

Yu, C.; Wang, X. & Qin, J. Effect of necrostatin-1 on sciatic nerve crush injury in rat models. *J. Orthop. Surg. Res., 18(1)*:74, 2023.

Zhang, T.; Li, Z.; Dong, J.; Nan, F.; Li, T. & Yu, Q. Edaravone promotes functional recovery after mechanical peripheral nerve injury. *Neural. Regen. Res., 9(18)*:1709-15, 2014.

Zhong, J.; Rao, X. & Rajagopalan, S. An emerging role of dipeptidyl peptidase 4 (DPP4) beyond glucose control: potential implications in cardiovascular disease. *Atherosclerosis, 226(2)*:305-14, 2013.

Corresponding author:
Rasha Mamdouh Salama
Department of Anatomy and Embryology
Faculty of Medicine
Menoufia University
Menoufia
EGYPT

E-mail: drrashasalama@yahoo.com
rasha.salama@med.menofia.edu.eg

Orcid ID: 0000-0001-7582-3851